Mesoporous silicon photonic crystal microparticles: towards single-cell optical biosensors†

Bin Guan,[a] Astrid Magenau,[b] Krisopher A. Kilian,[a] Simone Ciampi,[a] Katharina Gaus,[b] Peter J. Reece[c] and J. Justin Gooding*[a]

Received 12th May 2010, Accepted 11th June 2010
DOI: 10.1039/c005340f

In this paper we demonstrate the possibility of modifying porous silicon (PSi) particles with surface chemistry and recognition molecules (antibodies) such that these devices could potentially be used for single-cell identification or sensing. This is achieved by modifying PSi Rugate filters *via* hydrosilylation with surface chemistry that serves firstly, to protect the silicon surfaces from oxidation; secondly, renders the surfaces resistant to nonspecific adsorption of proteins and cells and thirdly, allows further functionality to be added such as the coupling of antibodies. The surface chemistry remained unchanged after sonication of the PSi to form PSi microparticles. The ability to monitor the spectroscopic properties of microparticles, and shifts in the optical signature due to changes in the refractive index of the material within the pore space, is demonstrated. The particles are shown to remain stable in physiological buffers and human blood for longer than one week. Finally, the modification of the PSi particles with functional antibodies is achieved.

1 Introduction

Porous silicon (PSi) is a particularly versatile material having found applications in photonic devices,[1] electrodes,[2] sensor systems[3] and drug-delivery devices.[4,5] Hence PSi also has potential to be applied in theranostics. Mesoporous silicon, where pores are in the size range of 2–50 nm, is the most relevant material for these applications. It is most commonly prepared by anodically etching the silicon in hydrofluoric acid (HF) in, effectively, a corrosion reaction,[2] where the silicon is first oxidised and the resultant SiO_2 is then dissolved away in the HF. Remarkably, under many conditions the corrosion commences at a nucleation site on the silicon surface and proceeds linearly through the material to result in a columnar pore. Importantly for the above-mentioned applications, the size of the pore, and hence the extent of porosity, can be easily tuned by controlling the current density, and hence the dissolution rate,[6] during formation. That is, the exquisite control over reactivity that electrochemistry provides is directly translated into the same exquisite control over the material's structure. It is this ability to control and alter porosity, and pore size, with nanoscale resolution as the PSi is being fabricated that allows one-dimensional

[a]*School of Chemistry, The University of New South Wales, Sydney, NSW, Australia. E-mail: justin.gooding@unsw.edu.au; Fax: +61-2-937585 6141; Tel: +61-2-9385 5384*
[b]*Centre for Vascular Research, The University of New South Wales, Sydney, NSW, Australia*
[c]*School of Physics, The University of New South Wales, Sydney, NSW, Australia*

† Electronic supplementary information (ESI) available: Chemical modification schemes, quantification of particle size distributions, additional FTIR spectra and stability studies of particles with optical signatures in the near-IR are presented. See DOI: 10.1039/c005340f

photonic crystals, with complicated multilayer structures, to be produced. High-quality optical structures such as Bragg reflectors,[7] microcavities[8] and Rugate filters[9] have been produced from PSi.

It is the optical structures formed from PSi that sees this material applied to sensing. The optical signature of the photonic crystals is sensitive to the average refractive index of the structure. Therefore, in sensing, the adsorption of material to the pore walls will cause a red-shift (to longer wavelengths) if it has a higher refractive index than the material it replaces because the average refractive index of the structure increases. Similarly, if this material desorbs from the pore walls, the average refractive index decreases, and there is a concomitant blue-shift (to shorter wavelengths). By modifying the pore walls with the appropriate surface chemistry, PSi photonic crystals can be turned into label-free optical detectors with the required selectivity for the analyte of interest.[3]

Apart from being a label-free system, PSi photonic crystals are particularly attractive for biosensing as the optical signature can be tuned, *via* changes in the porosity and periodicity of the multilayer photonic crystals, over the entire visible and infrared regions of the electromagnetic spectrum. Tuning the optical signature to the near-IR between 700–1000 nm is particularly attractive as transmission through tissue is then possible[10] and hence PSi may be amenable to implantable devices for non-invasive interrogation. Another aspect of PSi that makes it attractive for use in biological systems, such as *in vivo* applications, is that PSi has been shown to degrade in aqueous solution to orthosilicic acid by the following mechanisms:[11]

$$Si(s) + 2H_2O(l) \rightarrow SiO_2(s) + 2H_2(g)$$

$$SiO_2(s) + 2H_2O(l) \rightarrow Si(OH)_4(l)$$

As orthosilicic acid is the natural form of silicon found in the body it can be readily excreted *via* the kidneys[12] and has been shown to elicit a limited foreign body response that is comparable to titanium surfaces when implanted in rats.[4,13] Hence implanted devices will eventually degrade away and not require surgical removal. It is the degradation that sees PSi used as a material for drug delivery of poorly solubilised drugs.[4,5] With the drug incorporated into the pore space of the PSi, the effective solubility of poorly soluble drugs is increased while the degradation of the PSi in biological fluids enables controlled release of the drug. The issue here is, however, that the degradation of freshly etched PSi is rapid (within hours).[14] To slow the degradation down requires chemical modification of the PSi.

There are two main surface chemistries employed for the chemical modification of the PSi. One strategy is to thermally oxidise the PSi and then use classical silane chemistry.[3,15] This chemistry however does not effectively passivate the PSi from degradation in aqueous solutions and is prone to hydrolysis itself. Further, it is difficult to determine whether monolayers or multilayers have been formed.[3] The other common strategy is to exploit the fact that the freshly prepared PSi presents a hydrogen-terminated silicon surface. Linford and Chidsey[16,17] showed that alkenes and alkynes could be reacted with such surfaces to give very stable monolayers on silicon without an intervening oxide layer (Scheme 1). This surface chemistry does not suffer from the drawbacks of silane chemistry but it is challenging to modify silicon with this surface chemistry without some oxide forming.[18] Any oxide present will then cause the PSi to degrade in aqueous solution.[14,19,20] With regard to stabilising PSi for drug delivery, Canham and co-workers[21] showed that using the hydrosilylation of dodecene to modify PSi the material showed little degradation over four weeks. Note however, that as dodecene renders the material hydrophobic, part of the reason for the excellent stability enhancement is that little

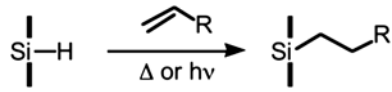

Scheme 1 A general representation of the hydrosilylation reaction used to modify hydrogen-terminated silicon surfaces with alkenes or alkynes with heat or UV light.

or no water penetrates into the pore space. More recently, we have shown that degradation is much more rapid in plasma if the modifying layer formed *via* hydrosilylation is hydrophilic.[14,19] However, the use of hydrophilic surface chemistry that resists protein adsorption, enhances the stability of PSi in plasma and biological buffers markedly. Modifying a PSi photonic crystal using undecenoic acid followed by the addition of an hexa(ethylene oxide) antifouling moiety allowed optical signatures from the photonic crystals to be recorded even 60 days after immersion in biological buffer.[14] Furthermore, we have shown that the degradation rate of PSi can be controlled by subtle variations in the coverage of the organic molecules attached to the PSi.[18]

Surface chemistry similar to that described above has also been crucial in our efforts to turn PSi photonic crystals into biosensors.[3] For biosensors, the surface chemistry is required not only to stabilise the device but also to give the photonic crystal the selectivity for the target analyte. Initial studies into using PSi for biosensing focussed on affinity sensors for the detection of DNA,[22,23] proteins[22,24,25] and microorganisms.[26] However, more recently there has been a trend to use PSi photonic-crystal-based biosensors for detecting enzymatic activity, specifically protease enzyme activity.[20,27–32] The focus of interest on protease enzymes was motivated by the importance of this class of enzyme in natural processes such as cell migration and tissue remodelling, as well as acting as a marker of many pathologies and infection, where early detection is often critical.[33]

Our main aim is to detect protease activity and hence cell activity for the development of responsive cell chips for diagnostic and theranostic purposes. Macrophage and other immune cells respond to environmental stimuli, such as chemical cues, chemokines, and the presence of foreign species, by releasing granules containing a high concentration of protease enzymes. The enzymes remodel the surrounding extracellular matrix, often leading to substantial tissue damage. Hence, monitoring the activity, and not just the presence of, protease enzymes serve as an excellent extracellular marker of the response of cells to their environment, of immune responses and cell activities that underlies a pathology.[34–36] To develop a chip that

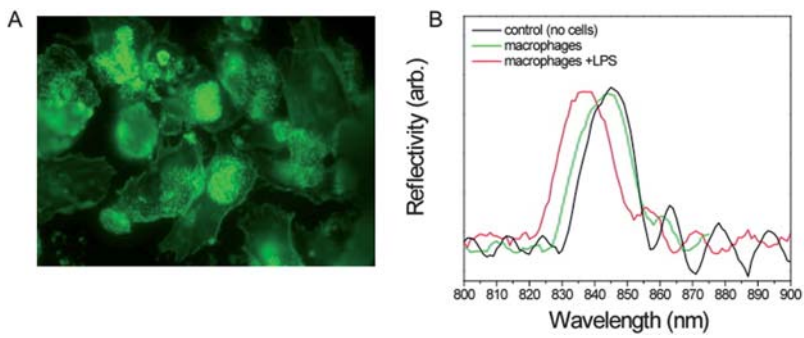

Fig. 1 PSi photonic crystals detect secretion of gelatinase enzymes. A) Human monocyte derived macrophages stained for actin adhere uniformly to gelatin coated PSi. B) After 24 h of lipopolysaccharide (LPS) stimulation the photonic resonance of the Rugate filter blue-shifts 8 nm, indicating digestion of the pore-encapsulated polypeptides.

can monitor protease release from specific cells requires a material that can capture the cells and, at the same time, monitor the release of protease enzymes from cells with the required sensitivity. This is where PSi comes in.

Using PSi we have 1) developed the surface chemistry to stabilise this material in biological buffers and plasma,[14,19,20] 2) shown that we can detect protease activity by attaching peptide substrates, for the protease enzymes, to the pore walls of the PSi,[20,27] 3) demonstrated that cell adhesion ligands can be attached onto the exterior of a PSi photonic crystal while different chemistry can be attached to the internal pores[37,38] and 4) that the release of protease enzymes from live cells captured onto the PSi surface could be detected *via* degradation of a gelatin substrate immobilised inside the pores of the PSi.[28,39] The types of data obtained using these four developments are shown in Fig. 1.

Here we used Rugate filters. Rugate filters are a class of photonic bandgap structures with a periodic sinusoidal refractive index profile. They are formed in PSi by modulating the porosity of the film on the sub-micrometre scale during etching. The structures are characterised by a spectral band of high reflectivity where the central wavelength (λ) is given by $\lambda = nd$, where n is the average refractive index and d is the physical thickness of each period. The width of the reflectivity is proportional to the amplitude of the refractive index modulation, and for small variations, the reflectivity band can be very sharp; of the order of 10 nm. Importantly, the corresponding porosity modulation means there is very little variation in porosity across a photonic crystal. For example, with the photonic crystals used in Fig. 1, the porosity varied between 64 and 66%, with pore diameters of 50 nm.[27] This essentially means the pore size is virtually unchanged through the structure and hence there will be little variation in the rate of mass transport of enzymes throughout the structure.

Fig. 1 shows the power of using these engineered PSi photonic crystals for cell chips. The adherence of human monocyte derived macrophages (HMDMs) to the PSi substrate is shown in Fig. 1A where cells are well spread on the substrate. Fig. 1B shows the change in the optical signature of the photonic crystals as a result of the release of matrix metalloproteases (MMPs) from the HMDMs. These optical responses are obtained from an estimated 1500 cells.[39] The blue-shift in the optical signature is a result of degradation of gelatin from the pores of the PSi, with lower-refractive-index water ($n \sim 1.3$) replacing the higher-refractive-index gelatin ($n \sim 1.4$). An increased response was seen as a larger blue-shift when the cells were exposed to LPS (a lipopolysaccharide found on the exterior of gram-negative bacteria) because the LPS triggers the release of MMP-2 and MMP-9 which are both gelatinases.[40,41] The number of cells that give the response shown in Fig. 1B was a consequence of the size of the footprint of the light source used to acquire the data rather than the sensitivity of the device. The measured sensitivity is actually determined by the proportion of pores in which gelatin was degraded and it was demonstrated that degradation of gelatin in only 1 in 30 pores is easily observed.[28] Hence, reducing the area of spectral collection down to the micrometre range should allow single-cell measurements to be performed.

The purpose of the present paper is to outline the progress made towards single-cell sensing using PSi Rugate filters. To achieve this in cell culture, we decided to form PSi microparticles and make them selective for specific cell types by modifying the particles with antibodies. The fabrication of PSi microparticles has most commonly been done by using a high current pulse to lift-off a PSi photonic crystal from the silicon wafer in which it was formed, and then shatter it into small pieces *via* sonication.[42–44] The PSi pieces have a broad distribution of sizes in the micrometre range of 4 to 80 μm (Figs. S1 & S2 of the ESI†). Extending our previous work on detecting protease activity in single-cell sensors requires a number of questions to be answered. These are: 1) Can we measure optical signatures from single particles and how reproducible are they? 2) How do we modify particles with surface chemistry to stabilise them and incorporate selectivity for a target analyte? An important

part of this question is to work out the sequence of fabrication steps *e.g.* is the protective surface chemistry best performed before the high current pulse in HF that is necessary to cause the lift-off from the silicon crystal, after lift-off but before formation of particles or after the formation of the particles? 3) How stable will the particles be in aqueous solution and biological buffers and how will the surface chemistry influence this? and 4) Can the particles be modified with antibodies such that their binding affinity is retained? The success of these developments is outlined below.

2 Experimental section

2.1 General

All chemicals, unless noted otherwise, were of analytical grade and used as received. Chemicals used in surface modification procedures were of high purity ($\geq$ 99%). 1,8-Nonadiyne (Alfa Aesar, 97%) was redistilled from sodium borohydride (Sigma-Aldrich, 99+%) under reduced pressure (79 °C, 8–9 Torr) and collected over activated molecular sieves (Fluka, 3 Å pore diameter, 10–20 mesh beads, dehydrated with indicator), and stored under a dry argon atmosphere prior to use. MilliQ™ water (>18 MΩ·cm) was used to prepare solutions and for chemical reactions. Dichloromethane, ethanol, and ethyl acetate for surface cleaning, chemical reactions and purification procedures, were redistilled prior to use. Dry acetonitrile was obtained from PureSolv MD 7 Solvent Purification System (Innovative Technology, Inc., Galway, Ireland). The azide compounds, 1-azido-octane and 11-azido-3,6,9-trioxaundecan-1-ol were synthesized as described previously.[38] Prime grade single-side polished silicon wafers, 100-oriented (<100> $\pm$ 0.05°), p-type (boron), 350 $\pm$ 25 μm thick, 0.069–0.077 Ω·cm resistivity, were obtained from M.M.R.C Pty. Ltd. (Malvern, VIC, Australia).

The antibodies, Cy3 AffiniPure donkey anti-rabbit IgG (H + L), Cy3 AffiniPure donkey anti-goat IgG (H + L) and Cy3 AffiniPure donkey anti-mouse IgG (H + L) were all purchased from Jackson ImmunoResearch (West Grove, PA, USA). Mouse-hosted FITC anti-human CD3 primary antibody was obtained from eBioscience (San Diego, USA).

2.2 Fabrication of porous silicon lift-off films

Rugate filters with 60 periods of low and high refractive index layers were prepared in a custom-made electrochemical cell with 1 : 1 by volume solution of 48% hydrofluoric acid/99% ethanol as described in ref. 9. A current density varying between 42 mA·cm^{-2} and 124 mA·cm^{-2} was applied periodically to afford a porous structure with a porosity variation from 54% to 64% and an average pore size of 20 nm (see Fig. S4†). After etching, a high current pulse (11.3 mA·mm^{-2}) was employed to lift the PSi structure off the substrate (but with the circumference of the PSi remaining attached to the substrate) with 1 : 2.3 by volume solution of 48% hydrofluoric acid/99% ethanol. The lift-off wafer was then rinsed with ethanol and pentane and dried with argon.

2.3 Chemical modification of porous silicon lift-off films

Stepwise modification of the PSi Rugate filter lift-off films followed a previously reported procedure.[38] Briefly, freshly etched filters were modified with neat 1,8-nonadiyne in a dry argon atmosphere at 170 °C for 3 h to form acetylene monolayers on the surface. The filters were then placed in a typical "click" reaction mixture consisting of: 1) the azide compound (10 mM, ethanol/water, 1 : 1 v/v); 2) copper(II) sulfate pentahydrate (1 mol % relative to the azide); 3) sodium ascorbate (25 mol % relative to the azide) for further modification. In the absence of a Cu(I)-stablizing ligand, *N*,*N*,*N*′,*N*′-tetramethylethane-1,2-diamine (TMEDA), the lift-off samples were functionalized with 11-azido-3,6,9-trioxaundecan-1-ol for 19 h to form tetra(ethylene

glycol) (EO_4) terminated surfaces on the exterior only. Modification of the interior pore surface with either 1-azido-octane or 11-azido-3,6,9-trioxaundecan-1-ol was followed an analogous procedure, but with 0.5% (v/v) TMEDA in the "click" mixture to afford either an octyl- or an EO_4-terminated interior. After each modification step, the PSi films were rinsed consecutively with ethanol and ethyl acetate and blown dry under a gentle stream of argon before further reaction.

2.4 Engineering of porous silicon microparticles

The PSi lift-off samples with different functionalities on the exterior and interior were floated off the substrate and placed in a 2-mL eppendorf tube with 1 mL ethanol for sonication. PSi microparticles in the size range of 4–80 μm were engineered in a Misonix Sonicator 2000 with a Microtipt™ probe (Qsonica, LLC. USA) at the energy of 266 J (amplitude 30) for 1 min with one repeat. The particles were dried under vacuum and stored under argon for further use.

2.5 Porous silicon microparticle stability test

Porous silicon microparticles at the size of around 10 μm were incubated in phosphate buffered saline (1× PBS, pH 7.4), Dulbecco's Modified Eagle Medium (DMEM) or a white blood cell concentrate from human blood (composed of mostly leukocytes and platelets and referred to as 'buffy coat') (diluted 1 : 5 v/v with 1× PBS) at 37 °C in 5% CO_2, while reflectivity measurements and epi-illumination micrographs were taken over time in solution.

2.6 Antibody functionalities on PSi particles

Tetra(ethylene glycol) EO_4-terminated PSi microparticles were placed in a reaction tube containing: a) *N*,*N*′-disuccinimidyl carbonate (DSC, 0.1 M) and b) *N*,*N*-dimethylaminopyridine (DMAP, 0.1 M) in dry acetonitrile for 20 h in the presence of activated molecular sieves (3 Å). The succinimidyl-terminated particles were rinsed with ethyl acetate and dichloromethane and then transferred to an antibody solution (1 : 500 v/v) in 1× PBS for 1 h at room temperature. Antibody-coupled PSi particles were then rinsed with MilliQ™ water and 1× PBS washing buffer with 0.5% (v/v) Tween 20 (Sigma-Aldrich) and stored in 1× PBS for antibody functional tests.

Antibody functionality tests were conducted in two ways: 1) to test the ability of antibodies to recognise protein-modified particles. Here, PSi microparticles were coated with mouse anti-human CD3 IgG-FITC and then incubated with either anti-goat IgG-Cy3 (1 : 500 v/v in 1× PBS) or with anti-mouse IgG-Cy3 (1 : 500 v/v in 1× PBS), respectively, for 1 h at room temperature; 2) to explore whether antibody-modified particles selectively bind to protein markers. PSi microparticles were coated with anti-rabbit IgG-Cy3 or with anti-mouse IgG-Cy3. The modified PSi particles were then incubated with mouse anti-human CD3 IgG-FITC-(1 : 500 v/v in 1× PBS). The particles were then rinsed twice with 1× PBS washing buffer (0.5% (v/v) Tween 20), followed by 1× PBS and stored in 1× PBS at 4 °C for fluorescence imaging.

2.7 Optical and surface characterisation

Optical reflectivity spectra of the microparticles were measured in the visible and near-IR at normal incidence using a custom-built optical arrangement on an inverted Leica DM IL LED microscope (Leica Microsystems Pty Ltd, USA). In this set-up a USB2000+ miniature fiber optic spectrometer (Ocean Optics Inc., USA), having a spectral resolution of 1 nm, was coupled to a multimode fibre with the collecting facet mounted in the conjugate image plane of the microscope. The microscope was equipped with a N PLAN L 40×/0.55 air objective, an epi-illumination brightfield slider and a ProgRes® CFscan camera (JENOPTIK Laser, Optik,

Systeme GmbH, Germany) for capturing the reflectance images of particles. The collecting aperture of the fibre-coupled spectrometer had a diameter of 100 μm which corresponded to an effective collecting spot of approximately 3 μm at the sample plane. Reflectivity spectra were recorded and processed using the SpectraSuite spectroscopy software platform (Ocean Optics Inc., USA).

Fluorescence images of particles in antibody function tests were obtained with the same Leica microscope, fitted with a mercury short-arc reflector lamp. FITC-fluorescence was detected with a excitation filter: BP470/40, a dichroic mirror: 500 and a emission filter: 525/50. Cy3 fluorescence was detected with a excitation filter: BP545/50, a dichroic mirror: 565 and a emission filter: 610/75. The images were recorded with the ProgRes Capture Pro 2.7 software (JENOPTIK Laser, Optik, Systeme GmbH, Germany) and processed with ImageJ 1.42q (National Institutes of Health, USA).

The Spotlight 400 Fourier transform infrared spectroscopy (FTIR) microscope system was from PerkinElmer and was used to record transmission FTIR spectra from single PSi particles. The particles were vacuum dried and mounted on a KCl disc. The spectra were then collected at the resolution of 2 cm^{-1} and an average of 128 scans with a light aperture of 45 × 45 μm.

Scanning electron microscopy (SEM) images were taken using a Hitachi S900 SEM with a cold-field emission source (4 kV). PSi microparticles were mounted on a brass sample base using carbon tape.

3 Results and discussion

3.1 Formation of porous silicon nanoparticles and their reflectivity spectra

Rugate filters were fabricated in single crystal, p-type, Si(100) with 60 layers and a pore size of 20 nm. After preparation, a high current pulse was used to cause a fracture between the crystalline silicon and the PSi sample. However, the lateral edges of the PSi remain attached to the silicon crystal. It is this partially attached PSi sample that is modified prior to particle formation according to scheme S1† as discussed below. After surface modification, the PSi lift-off sample was completely removed from the silicon crystal and converted into particles. After particle formation, it was important to demonstrate that reflectance spectra of individual particles could be monitored and that each particle from a batch exhibited a similar reflectivity spectrum. To take spectra of single particles, a normal epi-fluorescent microscope was

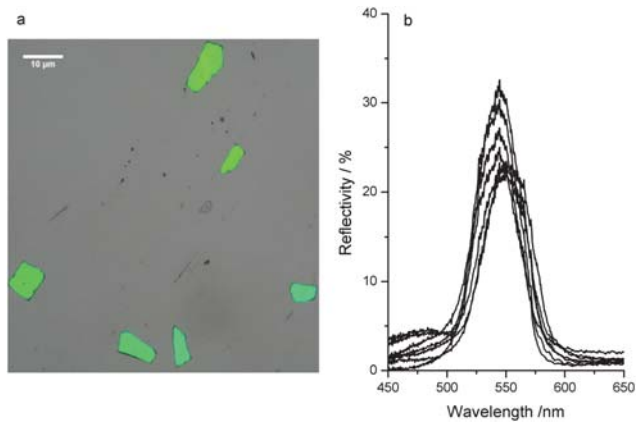

Fig. 2 a) Epi-illumination bright-field images of ethylene glycol modified PSi particles after sonication and b) reflectivity spectra of PSi particles from the same modified PSi film, featuring a high reflectivity peak at 547 ± 3 nm (mean ± SD).

employed where a collecting optical fibre mounted at the conjugate image plane in the camera port was used to record spectral data. The types of epi-illumination images of the particles and the reflectivity spectra of these particles are shown in Fig. 2.

As is evident from Fig. 2 there is some variation in the colour and spectra of these particles. This variation arises from slight differences in the fabrication of the Rugate filter across the sample due to uneven distribution of electrical field lines during the fabrication of the PSi. Importantly however, the optical properties are not significantly altered during sonication of the lift-off PSi sample to form particles.

3.2 Modification of porous silicon microparticles *via* hydrosilylation

Rather than first forming the particles and then modifying them, it was decided to use a high current pulse to partially detach the PSi from the silicon crystal on which it was formed and then modify the PSi before sonication, according to Scheme S1 of the ESI.† The reason for this was ease of handling but it did mean 1) that there would be unmodified silicon where the silicon was fractured and 2) that the surface chemistry was required to be capable of surviving the high energy of the sonication. As shown in Scheme S1 the PSi structure is first modified with the dialkyne, 1,8-nonadiyne, in an inert atmosphere at 170 °C for three hours. Subsequently, further functionality is added by reacting an azide-bearing moiety with the distal alkyne in the presence of a Cu(I) catalyst *via* the Huisgen 1,3-dipolar cycloaddition reaction; the archetypal 'click' reaction. It has been shown previously that this surface chemistry provides excellent protection of the underlying silicon surface from oxidation, even under anodic potentials,[45] with both flat silicon[46] and PSi.[47] We note that in our hands it was much easier to produce good protection of PSi from oxidation using this 1,8-nonadiyne than the chemistry we used previously that employed undecenoic acid.[3] Furthermore, although unnecessary on flat silicon, for the 'click' reaction to proceed within mesoporous silicon requires the complexation of the Cu(I) catalyst with a *N*,*N*,*N*′,*N*′-tetramethylethane-1,2-diamine ligand for the reaction to proceed inside the pores.[47] This observation was used to modify PSi with completely different chemistry inside the pore space relative to the exterior surface[38] as shown using optical reflectivity, X-ray photoelectron spectroscopy (XPS) and transmission Fourier transform infrared (FTIR) spectroscopy.[2] Using this strategy, the exterior surface was modified with an azido tetra(ethylene glycol) to render the external surface resistant to nonspecific protein and cell adsorption but also to allow further attachment

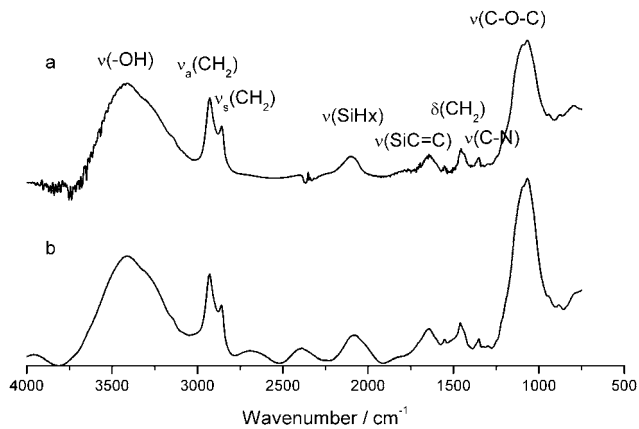

Fig. 3 Comparison of FTIR spectra of porous structure modified with alkyne monolayers and EO_4 moieties inside and out in lift-off PSi films (a) before sonication, and (b) in PSi particles after sonication.

of biomolecules to the alcohol terminus of this molecule as described previously.[48] The internal pore surfaces were then modified with the same tetra(ethylene glycol) species to make the internal surface hydrophilic, such that water will easily penetrate the pores, and to allow attachment of the gelatin substrate required by matrix metalloprotease enzymes secreted from macrophage cells (MMP-2 and MMP-9). Alternatively the internal pores were modified with an octane species to make the internal volume hydrophobic.[37] The reason for this modification was to explore whether better stability of particles in biological media was achieved if the ingress of aqueous solution into the material was limited.

After modifying the PSi with the base 1,8-nonadiyne layer followed by clicking on different functionality to the internal and external surfaces, the PSi disk was cut from the silicon crystal and sonicated in ethanol to give micrometre-size particles. To show the surface chemistry was not altered by the highly energetic conditions of sonication transmittance FTIR was performed before and after the sonication step (Fig. 3).

Fig. 3a shows the asymmetrical and symmetrical stretching of the CH_2 group at 2925 cm^{-1} and 2852 cm^{-1} remains unchanged. The broad OH stretch in the range 3500–3200 cm^{-1} and C–O stretching vibration at 1150 cm^{-1} support the presence of ethylene glycol moieties on the surface. Also present are the bands at 1630 cm^{-1}, 1455 cm^{-1} and 1350 cm^{-1}, ascribed to Si–C=C stretching, CH_2 scissoring and C–N bond respectively, strongly supporting a complete surface modification on PSi particles. Significantly, there is no broad band around 1150 cm^{-1} which would be indicative of any silicon oxide, thus indicating the effectiveness of the surface chemistry at modifying the silicon without any silicon oxides being formed. Most importantly however, Fig. 3a and b show no discernable difference indicating the sonication did not cause any harm to the surface chemistry. Similar results are

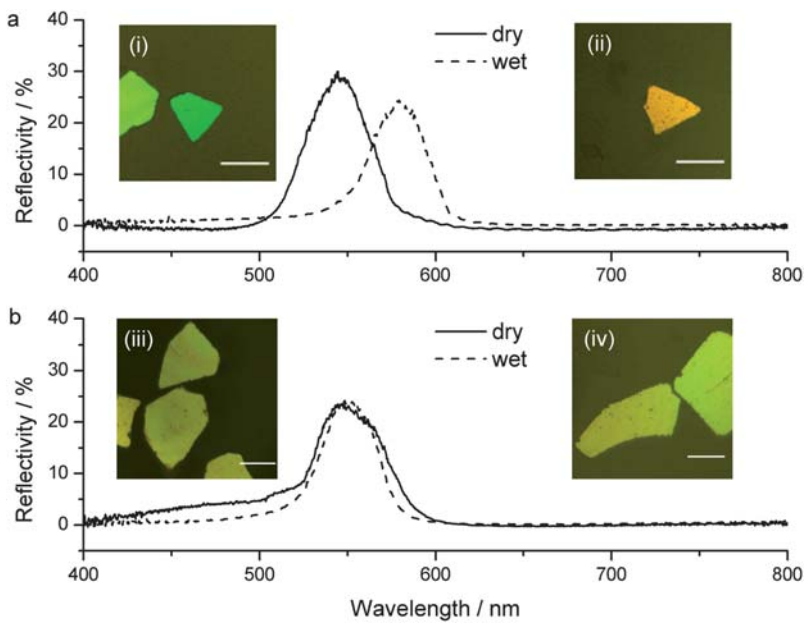

Fig. 4 PSi particles with hydrophilic and hydrophobic internal functionalities in dry/wet conditions. (a) Reflectivity spectra of a single hydrophilic particle in air and in phosphate-buffered saline (PBS). A color change from green (i) to red (ii) in the same hydrophilic particle can be observed. (b) Reflectivity spectra of a hydrophobic particle in air and in PBS. The insets (iii) and (iv) show the illumination images of hydrophobic particles in dry and wet conditions, respectively. Scale bar equals 50 μm.

observed when the internal surface chemistry is terminated with octyl moieties (see Fig. S3 of the ESI†).

The effectiveness of the surface modification in controlling the way the particles interacted with aqueous solution, and hence a demonstration of the ability to place different surface chemistry on the inside and outside of the PSi particles, was demonstrated using reflectivity measurements. The particle with internal octane-terminations are expected to exclude water from penetrating into the pores, while with a hydrophilic group, *e.g.* ethylene glycol, the pores are expected to be filled with water. As water has a higher refractive index than the air it replaces, the penetration of water into the structure will result in a red-shift in the reflectivity peak to longer wavelengths. Photonic crystals with reflectivity bands in the visible region were employed for this purpose so the changes could also be seen visually (Fig. 4). Fig. 4a shows a 30 nm spectral shift in the reflectivity spectrum caused by water infiltration and the two inset graphs [(i) & (ii)] display an abrupt color change of the same particle. No significant spectral shift in Fig. 4b suggests a well-passivated hydrophobic surface in the pores of PSi particles, which resist infiltration of water into the pore spaces.

3.3 Stability of PSi particles under physiological conditions

The next step was to evaluate the different particles, those with hydrophilic modification inside the pores and those with hydrophobic surface chemistry, for their stability in physiological media. We have performed such studies for similar hydrophilic surface chemistry with porous silicon still incorporated within the single crystal silicon and showed that PSi structures gave recognisable optical signatures for up to 60 days incubation in PBS buffer at 37 °C.[14,19] The particles however may have significantly lower stability because the fabrication of the particles exposed unmodified silicon that could then act as the site where degradation begins. The evaluation of the influence of physiological condition, and potentially an *in vivo* environment, on the PSi particles were performed in three different solutions: PBS, cell culture medium DMEM and diluted human blood buffy coat at physiological temperature and pH for up to 23 days.

Fig. 5 shows the reflectivity stop-band shift of PSi particles with hydrophobic octane groups inside the pores incubated in PBS (a), DMEM (b) and diluted human blood buffy coat (c), respectively. As there is some variation in optical properties between particles, for each time point more than 10 particles were evaluated and the spectral data from all particles are included in the figures. It is also important to recognise that the data at each time point come from the same population of particles but, as it is difficult to identify individual particles, the data at each time point does not necessarily come from the same particles as previous time points. What is apparent from all three media is that there is a red-shift of the reflectance band after a few hours which indicates water is penetrating the pores despite the pore surface chemistry being hydrophobic. This suggests that any protection of the particles from degradation will arise from the surface chemistry rather than the exclusion of water. After the initial red-shift, however, the central wavelength of the reflectivity peak remained statistically the same for up to 11 days in PBS and human blood. In the case of the cell culture medium, DMEM, the optical properties of the particles remain stable for 7 days whereupon a blue-shift in the reflectivity peak appears to suggest the particles are beginning to degrade, although distinct optical signatures are still easily discernable after 23 days. Also shown in Fig. 5b are optical micrographs of particles at different times during their incubation in the DMEM to visually illustrate the change in optical properties of particles.

The PSi particles functionalized with hydrophilic ethylene glycol moieties were also evaluated for stability in the same three media: PBS, DMEM and human blood buffy coat (Fig. 6). Unlike the hydrophobic particles there was no initial red-shift in

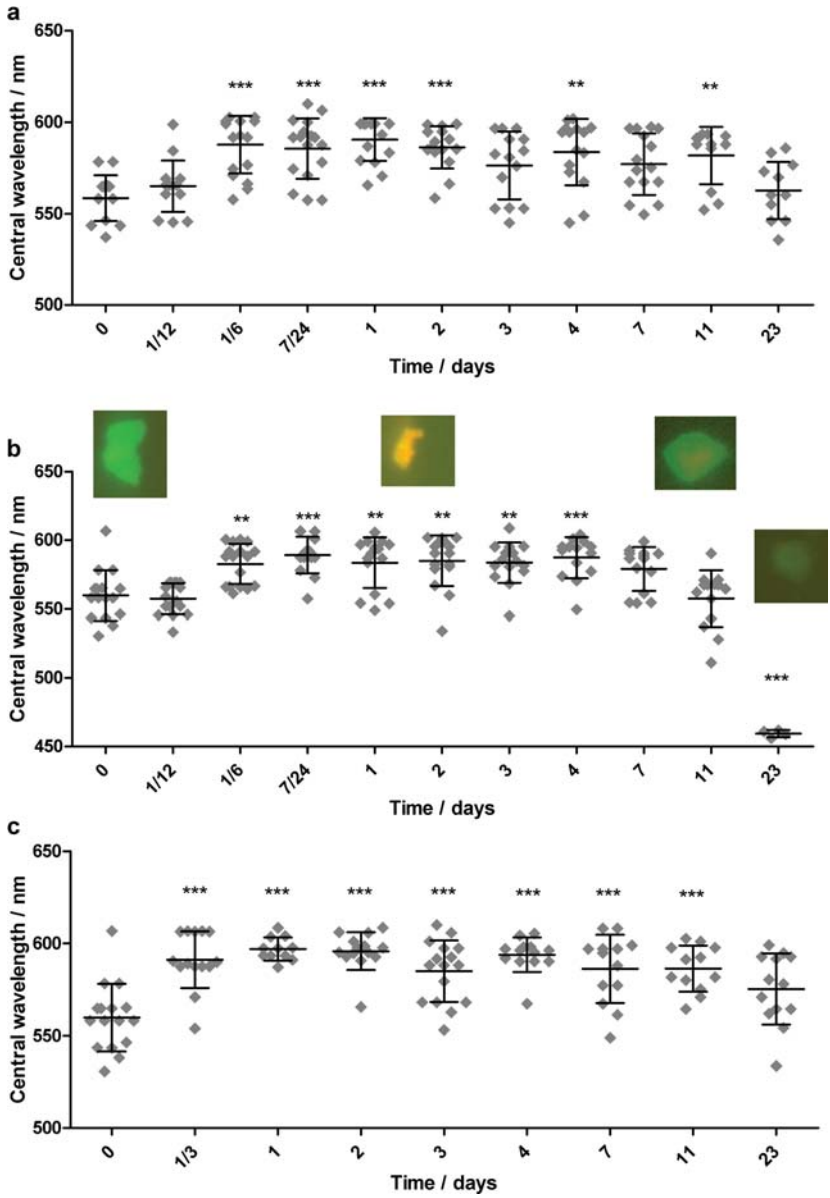

Fig. 5 Stability of the high reflectivity peak position for PSi particles with hydrophobic internal pores exposed to PBS (a), DMEM (b) and diluted human blood buffy coat(c) over time. The asterisks stands for the significance level of variances relative to the starting point (time 0) based on one-way ANOVA analysis: *** (99.9% confidence), ** (99% confidence) and * (95% confidence). The insets are illumination images of PSi particles at different incubation times in DMEM.

the reflectivity as the pore spaces of the particles were already filled with water. A gradual blue-shift in the position of the reflectivity band, presumably due to oxidation of the silicon and hence a degradation of the particles, was observed after two-day incubation in PBS (Fig. 6a). Similar results were shown for incubations in DMEM in Fig. 6b with the blue-shift becoming statistically significant after four

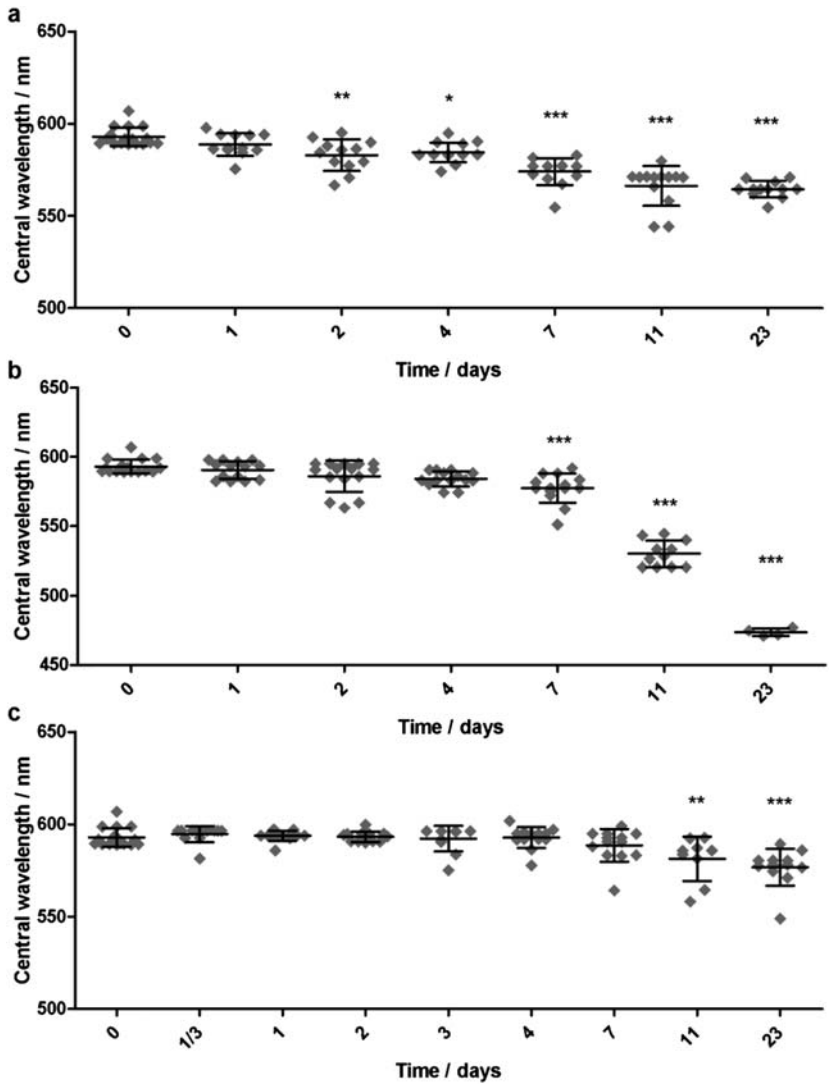

Fig. 6 Stability of the high reflectivity peak position for PSi particles with hydrophilic internal pores exposed to PBS (a), DMEM (b) and diluted human blood buffy coat (c) over time. The asterisks stands for the significance level of variances related to the start point (time 0) based on a one-way ANOVA analysis: *** (99.9% confidence), ** (99% confidence) and * (95% confidence).

days. In blood, Fig. 6c, the blue-shift, indicative of particle degradation, only became significant after more than one week. For comparison, the same stability tests were also performed on particles with hydrophilic interiors and exteriors, as in Fig. 6, but for particles with optical signatures tuned in the near-IR (the 'tissue window'). The near-IR particles showed virtually identical behaviour to those in Fig. 6 above (see Fig. S4 of the ESI†).

The stability studies were very encouraging as they show there is no major degradation of particles within the first few days of exposing them to physiological media which is well beyond the expected operation time for most diagnostic and

theranostic applications. Furthermore, it is clear that the particles will still provide some optical information for 23 days after application.

3.4 Antibody immobilization on PSi microparticles

The final questions explored in this study were whether particles could be modified with antibodies on the external surface and whether the antibodies maintained their functionality? Initial attempts to modify the exterior surface of the PSi with antibodies prior to sonication of the PSi lift-off sample to form the microparticles resulted in destruction of the antibodies. As a consequence, modified PSi particles were first prepared with a hydrophobic internal pore surface chemistry and a tetra (ethylene glycol) species on the external surface as shown in Scheme 2. The lift-off PSi was then sonicated to form particles; a process shown above not to affect the surface chemistry. The distal alcohol moieties on the tetra(ethylene glycol) were converted to succinimide esters using DSC/DMAP,[48] which then allows covalent coupling of amines such as those found on lysine residues of antibodies (Scheme 2). A fluorescence labeled antibody, cyanine 3 affiniPure donkey anti-mouse IgG (H + L) was chosen to test the antibody immobilization by examining its fluorescence under the Leica microscopy. The immobilization steps were further monitored using a transmission-mode FTIR microscope that was able to measure spectra from each single microparticle.

FTIR spectra obtained from ethylene glycol-terminated PSi particles, DSC-activated and antibody-coupled particles are shown in Fig. 7. The presence of $\nu_a(CH_2)$, $\nu_s(CH_2)$, $\delta(CH_2)$, ν(C–N) and ν(C–O–C) modes at 2925 cm^{-1}, 2852 cm^{-1}, 1455 cm^{-1}, 1350 cm^{-1} and 1150 cm^{-1}, respectively, in Fig. 7a verifies the PSi particles have been modified with ethylene glycol moieties, as shown before. The appearance of IR stretching at 1750 cm^{-1} in Fig. 7b, ascribed to C=O, suggests successful activation of the distal hydroxyl group of tetra(ethylene glycol) to a succinimide ester. After incubating the activated particles in the anti-mouse IgG antibody solution for 2 h, the stretching of the C=O bond disappeared. Instead, two broad peaks at 3380 cm^{-1} and 1680 cm^{-1} appeared pointing to the presence of polypeptides, indicative of anti-mouse IgG coupling on the PSi particles. In detail, there were two main peaks related to peptides around the wavenumber of 3400 cm^{-1}: one at 3454 cm^{-1} which is from the free N–H stretch vibration and another peak at 3330 cm^{-1} from the hydrogen-bonded N–H stretch vibration.

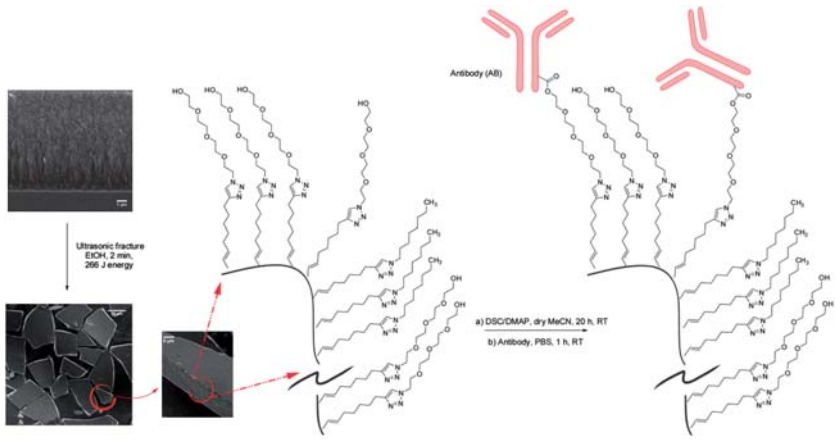

Scheme 2 The formation of PSi Rugate filter microparticles and the surface chemistry used to modify the microparticles with antibodies on the exterior surface.

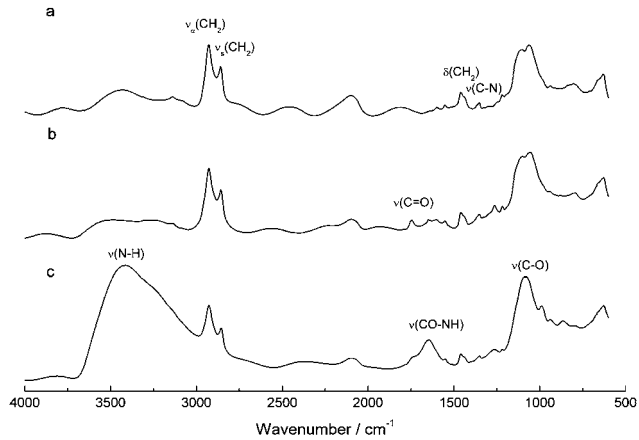

Fig. 7 Transmission-mode FTIR spectra of PSi microparticles at each step of immobilization. (a) PSi particles with distal ethylene glycol groups on the exterior and distal octane groups inside the pores. (b) DSC/DMAP-activated PSi particles. (c) Cy3-labeled antibody-coupled PSi particles.

Fluorescence images of PSi particles in Fig. 8 also support the successful immobilization of Cy3-labeled antibody through covalent bonding. The micrographs in Fig. 8a and b were taken from the same particles, but under different imaging modes: fluorescence and white light epi-illumination, respectively. The fluorescence images (Fig. 8a) show Cy3-labelled antibody across the entire PSi surface although it is noted that there seems to be a higher density of antibody at the particle edges. The particle edges are bare silicon, where no nonspecific protein adsorption resistant chemistry is located, and hence the high fluorescence intensity may reflect nonspecific adsorption of the antibodies.

Fig. 8 illustrates that antibody is immobilised onto the PSi microparticles but provides no evidence of antibody functionality. To assess the binding capabilities of surface-bound antibodies, the binding of free secondary antibody (AB^2) to recognize primary antibody-modified particles was examined here. In the method 1 of antibody functionality test, mouse FITC-labeled anti-human CD3 primary antibody was first covalently coupled onto PSi particles by the same chemistry approach in Scheme 2. The particles were then incubated with two types of secondary antibody (AB^2): cyanine 3 affiniPure donkey anti-mouse IgG that should selectively bind to the surface-bound, mouse anti-human CD3 primary antibodies and Cy3 AffiniPure

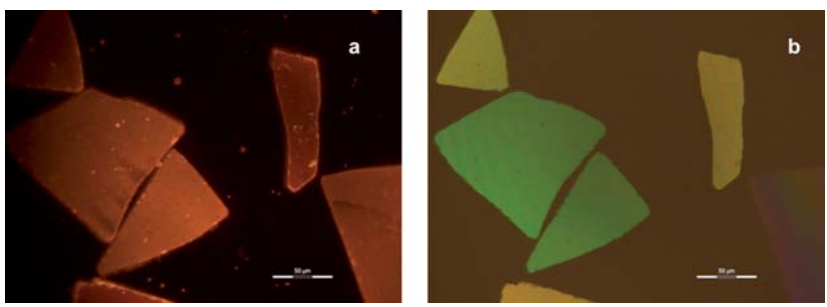

Fig. 8 (a) Fluorescence images of anti-mouse Cy3-labeled particles and (b) epi-illumination images of the anti-mouse Cy3-labeled particles.

donkey anti-goat IgG as a control that should have no specific affinity for the surface-bound antibodies.

Fluorescence images of the particles incubated with two different AB^2 were taken using a Leica DM IL microscope with a Cy3 filter and were quantified to compare the fluorescence intensities, shown in Fig. 9. Both anti-goat and anti-mouse AB^2-incubated particles show some fluorescence (Fig. 9a and b), indicating some nonspecific binding of anti-goat AB^2 onto the PSi particles. However, based on a one-way ANOVA analysis, anti-mouse AB^2-bound particles have significantly higher fluorescence intensity than the control particles with anti-goat AB^2 (Fig. 9c), in accordance with the fact that only anti-mouse AB^2 can specifically bind to the mouse-hosted anti-human CD3 primary antibody. This result serves as a demonstration that the binding epitopes of proteins immobilised on the PSi particles are preserved for binding to other proteins, an essential criterion for targeting specific cell types.

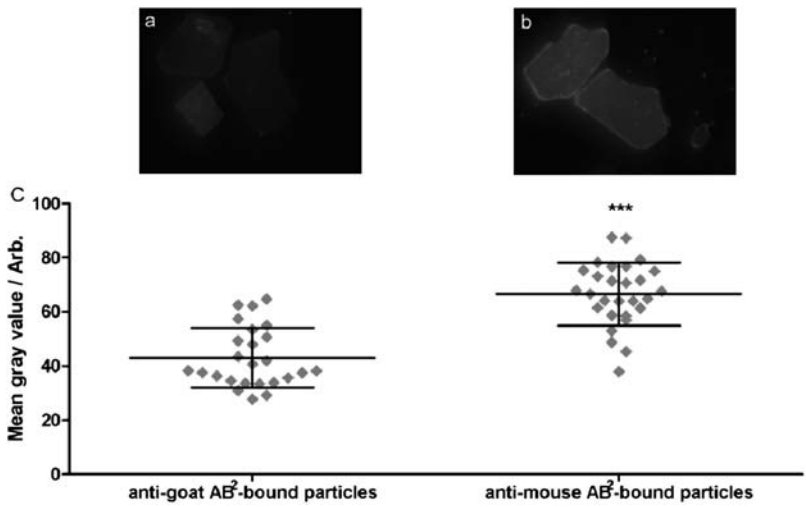

Fig. 9 Comparison of the fluorescence intensities from anti-goat AB^2-bound PSi particles and anti-mouse AB^2-bound particles. (a) and (b) fluorescence images of PSi particles with anti-goat AB^2 and anti-mouse AB^2, respectively. (c) Statistical analysis of fluorescence emissions by antibody-bound particles. The asterisks represent significant difference based on a one-way ANOVA analysis, while *** stands for significance at 99.9% confidence interval.

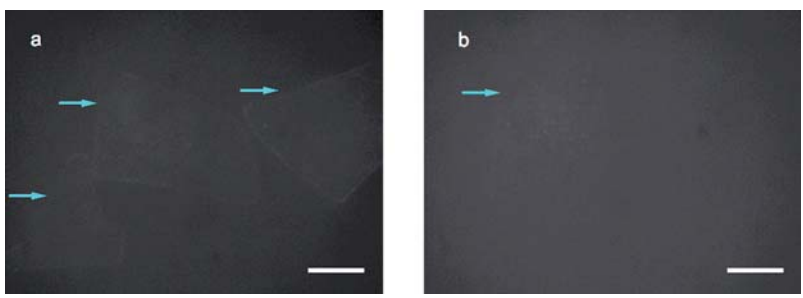

Fig. 10 Comparison of the green fluorescence images (in black and white mode) from FITC-labeled mouse anti-human CD3 AB-incubated PSi particles, which were modified with anti-mouse AB^2 (a) and anti-rabbit AB^2 (b), respectively. Arrows display the position of particles. Scale bar equals 50 μm.

To illustrate that antibodies bound to the particles remain capable of binding to specific epitopes of cells, a second antibody test was performed. In method 2, secondary antibodies, either Cy3-labeled anti-mouse AB^2 or Cy3-labeled anti-rabbit AB^2 were immobilised on the PSi particle surface first for selective binding to free primary antibodies in the solution. Fig. 10 shows the fluorescence micrographs of two different AB^2-modified PSi particles after incubating with FITC-labeled mouse anti-human CD3 primary antibodies. With anti-mouse AB^2, which specifically binds the FITC-labeled anti-human CD3 primary antibody, the particles showed brighter fluorescence than the reference ones with anti-rabbit AB^2 which have no specific affinity for the FITC-labeled anti-human CD3 primary antibody. Hence, this supported that the active binding sites on surface-bound antibodies maintain their functionality.

4. Conclusions

The recent demonstration that porous silicon photonic crystals could be functionalised such that they capture cells[32] and monitor the release of metalloprotease enzymes from living macrophage cells[26] highlighted the potential of this material as a diagnostic/theranostic tool. This initial work showed label-free detection of the release of enzymes from approximately 1500 cells but the concept could therortically be applied to single-cell sensing. Here we have outlined the realisation of many of the developments required to apply these ideas to single-cell sensing. Here, we use a similar strategy as the original study by Kilian *et al.*[34] but applied it to PSi particles. It was necessary to show that the PSi particles could be chemically modified such that the particles were stable in physiological media and could have functional biorecognition molecules attached to give them selectivity for target cell types. The fact that the PSi particles remained stable in physiological media for over one week and that antibody-modified particles maintained the ability to selectively bind their antigen illustrates that they can be used for the target application.

The study presented here takes us towards being able to perform selective binding of PSi particles to single cells and monitor the release of protease enzymes from these cells. To achieve the latter will require modifying the internal pore spaces of the PSi particles with an enzyme-specific substrate, as we have done for macroscale pieces of PSi. As the release of protease enzymes is up- or down-regulated by chemical agents, such as therapeutics, these PSi particles could be used for monitoring the impact of specific therapeutics on cell behaviour. This capability could then be used for monitoring drug efficacy and could be tailored to the cells of individuals, thus providing patient specific information of the drug action and dosage requirements; the very essence of theranostics.

Acknowledgements

The authors thank the Australian Research Council (project number DP1094564) and the National Health and Medical Research Council (project grant 630545) for support.

References

1 M. Gal, P. J. Reece, W. H. Zheng and G. Lerondel, in *Photonics: Design, Technology, and Packaging*, ed. C. Jagadish, K. D. Choquette, B. J. Eggleton, B. D. Nener and K. A. Nugent, SPIE, Bellingham, 2003, pp. 9–16.
2 G. X. Zhang, *Electrochemistry of silicon and its oxides*, Kluwer Academic, New York, 2001.
3 K. A. Kilian, T. Boecking and J. J. Gooding, *Chem. Commun.*, 2009, 630–640.
4 C. A. Prestidge, T. J. Barnes, C. H. Lau, C. Barnett, A. Loni and L. Canham, *Expert Opin. Drug Delivery*, 2007, **4**, 101–110.
5 E. J. Anglin, L. Y. Cheng, W. R. Freeman and M. J. Sailor, *Adv. Drug Delivery Rev.*, 2008, **60**, 1266–1277.

6 L. Canham and Editor, *Properties of Porous Silicon*, IEE, London, 1997.
7 W. H. Zheng, P. Reece, B. Q. Sun and M. Gal, *Appl. Phys. Lett.*, 2004, **84**, 3519–3521.
8 P. J. Reece, G. Lerondel, W. H. Zheng and M. Gal, *Appl. Phys. Lett.*, 2002, **81**, 4895–4897.
9 S. Ilyas, T. Bocking, K. Kilian, P. J. Reece, J. Gooding, K. Gaus and M. Gal, *Opt. Mater.*, 2007, **29**, 619–622.
10 S. J. Matcher, M. Cope and D. T. Delpy, *Appl. Opt.*, 1997, **36**, 386–396.
11 L. T. Canham, *Adv. Mater.*, 1995, **7**, 1033–1037.
12 D. M. Reffitt, R. Jugdaohsingh, R. P. H. Thompson and J. J. Powell, *J. Inorg. Biochem.*, 1999, **76**, 141–147.
13 A. Rosengren, L. Wallman, M. Bengtsson, T. Laurell, N. Danielsen and L. M. Bjursten, *Phys. Status Solidi A*, 2000, **182**, 527–531.
14 K. A. Kilian, T. Bocking, K. Gaus, M. Gal and J. J. Gooding, *Biomaterials*, 2007, **28**, 3055–3062.
15 B. E. Collins, K.-P. S. Dancil, G. Abbi and M. J. Sailor, *Adv. Funct. Mater.*, 2002, **12**, 187–191.
16 M. R. Linford and C. E. D. Chidsey, *J. Am. Chem. Soc.*, 1993, **115**, 12631–12632.
17 M. R. Linford, P. Fenter, P. M. Eisenberger and C. E. D. Chidsey, *J. Am. Chem. Soc.*, 1995, **117**, 3145–3155.
18 O. Seitz, T. Bocking, A. Salomon, J. J. Gooding and D. Cahen, *Langmuir*, 2006, **22**, 6915–6922.
19 K. A. Kilian, T. Bocking, S. Ilyas, K. Gaus, W. Jessup, M. Gal and J. J. Gooding, *Adv. Funct. Mater.*, 2007, **17**, 2884–2890.
20 T. Böcking, K. A. Kilian, K. Gaus and J. J. Gooding, *Adv. Funct. Mater.*, 2008, **18**, 3827–3833.
21 L. T. Canham, C. L. Reeves, J. P. Newey, M. R. Houlton, T. I. Cox, J. M. Buriak and M. P. Stewart, *Adv. Mater.*, 1999, **11**, 1505–1507.
22 V. S. Y. Lin, K. Motesharei, K.-P. S. Dancil, M. J. Sailor and M. R. Ghadiri, *Science*, 1997, **278**, 840–843.
23 S. Chan, P. M. Fauchet, Y. Li, L. J. Rothberg and B. L. Miller, *Phys. Status Solidi A*, 2000, **182**, 541–546.
24 K.-P. S. Dancil, D. P. Greiner and M. J. Sailor, *J. Am. Chem. Soc.*, 1999, **121**, 7925–7930.
25 H. Ouyang, L. A. DeLouise, B. L. Miller and P. M. Fauchet, *Anal. Chem.*, 2007, **79**, 1502–1506.
26 S. Chan, S. R. Horner, P. M. Fauchet and B. L. Miller, *J. Am. Chem. Soc.*, 2001, **123**, 11797–11798.
27 K. A. Kilian, T. Boecking, K. Gaus, M. Gal and J. J. Gooding, *ACS Nano*, 2007, **1**, 355–361.
28 K. A. Kilian, L. M. H. Lai, A. Magenau, S. Cartland, T. Bocking, N. Di Girolamo, M. Gal, K. Gaus and J. J. Gooding, *Nano Lett.*, 2009, **9**, 2021–2025.
29 M. M. Orosco, C. Pacholski, G. M. Miskelly and M. J. Sailor, *Adv. Mater.*, 2006, **18**, 1393–1396.
30 L. Z. Gao, N. Mbonu, L. L. Cao and D. Gao, *Anal. Chem.*, 2008, **80**, 1468–1473.
31 L. Gu, M. Orosco and M. J. Sailor, *Phys. Status Solidi A*, 2009, **206**, 1374–1376.
32 M. M. Orosco, C. Pacholski and M. J. Sailor, *Nat. Nanotechnol.*, 2009, **4**, 255–258.
33 C. Chang and Z. Werb, *Trends Cell Biol.*, 2001, **11**, S37–S43.
34 C. T. N. Pham, *Int. J. Biochem. Cell Biol.*, 2008, **40**, 1317–1333.
35 J. D. Raffetto and R. A. Khalil, *Biochem. Pharmacol.*, 2008, **75**, 346–359.
36 G. A. Rosenberg, *Lancet Neurol.*, 2009, **8**, 205–216.
37 K. A. Kilian, T. Bocking, K. Gaus and J. J. Gooding, *Angew. Chem., Int. Ed.*, 2008, **47**, 2697–2699.
38 B. Guan, S. Ciampi, G. Le Saux, K. Gaus, P. J. Reece and J. J. Gooding, *Langmuir*, 2010, submitted.
39 K. Kilian, A. Magenau, T. Böcking, K. Gaus, M. Gal and J. J. Gooding, *Proc. SPIE*, 2009, **7397**, 739703.
40 P. J. Bergin, S. Wen, Q. Pan-Hammarström and M. Quiding-Järbrink, *FEMS Immunol. Med. Microbiol.*, 2005, **45**, 159–169.
41 B. Xie, Z. Y. Dong and I. J. Fidler, *J. Immunol.*, 1994, **152**, 3637–3644.
42 J. L. Heinrich, C. L. Curtis, G. M. Credo, K. L. Kavanagh and M. J. Sailor, *Science*, 1992, **255**, 66–68.
43 J. R. Link and M. J. Sailor, *Proc. Natl. Acad. Sci. U. S. A.*, 2003, **100**, 10607–10610.
44 M. J. Sailor and J. R. Link, *Chem. Commun.*, 2005, 1375–1383.
45 S. Ciampi, P. K. Eggers, G. Le Saux, M. James, J. B. Harper and J. J. Gooding, *Langmuir*, 2009, **25**, 2530–2539.
46 S. Ciampi, T. Böcking, K. A. Kilian, M. James, J. B. Harper and J. J. Gooding, *Langmuir*, 2007, **23**, 9320–9329.
47 S. Ciampi, T. Böcking, K. A. Kilian, J. B. Harper and J. J. Gooding, *Langmuir*, 2008, **24**, 5888–5892.
48 T. Böcking, K. A. Kilian, T. Hanley, S. Ilyas, K. Gaus, M. Gal and J. J. Gooding, *Langmuir*, 2005, **21**, 10522–10529.